NASA Technical Memorandum 81504

QCSEE UTW Engine Powered-Lift Acoustic Performance

I.J. Loeffler, N.E. Samanich,
and H.E. Bloomer
Lewis Research Center
Cleveland, Ohio

Prepared for the
Sixth Aeroacoustics Conference
sponsored by the American Institute of Aeronautics and Astronautics
Hartford, Connecticut, June 4-6, 1980

NASA

QCSEE UTW ENGINE POWERED-LIFT ACOUSTIC PERFORMANCE

by I. J. Loeffler, N. E. Samanich, and H. E. Bloomer

E-442

INTRODUCTION

Powered-lift acoustic tests of the Quiet Clean Short-Haul Experimental Engine (QCSEE)[1,2] under-the-wing (UTW) engine were conducted by the NASA Lewis Research Center from May through November of 1979. The engine was tested in a static garound test facility with wing and flap segments to simulate an inboard engine installation on a short-haul transport aircraft. The results of these tests are reported in this paper. In addition, the UTW engine powered-lift acoustic performance is compared with that of the previously tested and reported QCSEE over-the-wing (OTW) engine.[3]

The QCSEE program was directed toward the development of propulsion system technology suitable for future short-haul powered-lift transport aircraft. A major objective of the program was the development of a very-low-noise propulsion system technology.

Propulsion systems for two powered-lift concepts were designed, fabricated, and static ground tested under NASA contract by the General Electric Company. One engine was designed for UTW mounting (Fig. 1), while the other was designed for OTW installation (Fig. 2). The UTW engine in the powered-lift mode is an example of an externally blown flap (EBF) system while the OTW engine in powered-lift operation is often called an upper-surfce blowing (USB) system.

The QCSEE engines were designed to meet very challenging noise goals. A 95-EPNdB goal was established on a 152-meter (500-ft) sideline for powered-lift takeoff and approach on a 610-meter (2000-ft) runway at the altitude at which maximum noise is produced. The noise goals are illustrated in Fig. 3. To meet these goals, the two acoustic designs featured a balance between the two major contributors; the jet-flap interaction noise (associated with powered-lift), and the combined internal engine noise.

Engine design parameters were selected to favor low source noise generation (see Table 1). Low jet-flap interaction noise requires low engine exhaust velocities. Consequently, low fan and core pressure ratios and high bypass ratios in the 10-to-12 range were selected to provide low exhaust velocities. For the reduction of engine internally generated noise and its transmission to the far-field, significant QCSEE engine features are also identified in Figs. 1 and 2. Engine source noise was also kept to a minimum by the low fan and core pressure ratios, and by the low fan tip speeds. The large rotor-stator spacing values, 1.5 for the UTW engine and 1.93 for the OTW engine, produce low rotor-stator interaction noise.

Advanced acoustic suppression concepts employed in both engines included a hybrid inlet (0.79 throat Mach number with acoustic treatment), high and low frequency "stacked" core noise treatment, multiple thickness fan inlet and fan exhaust duct treatment, an acoustically treated fan exhaust duct splitter, and fan frame and stator vane acoustic treatment. Further details of the QCSEE acoustic designs are given in Refs. 4 to 9.

To aid in achieving low noise with minimal performance penalties, composite structures were widely employed, particularly in the UTW engine, for engine weight reduction and for their potential cost savings. In the UTW engine, the engine frame, the fan blades, and the engine nacelle were of composite construction. The acoustic treatment, also of composite materials, was integrated into the load-carrying structure in the UTW engine nacelle for additional nacelle weight savings. The UTW engine also featured a variable-pitch fan which provided a reverse thrust capability as well as a quick thrust response for aborted landings. For optimal engine performance under all operating conditions, and particularly during forward and reverse thrust transient operation, an automatic digital control was designed and built for this engine. The OTW engine employed a composite fan frame, a fixed-pitch fan, a higher fan pressure ratio, and a full-authority digital control system.

At the conclusion of testing by General Electric, both engines were delivered to the NASA Lewis Research Center for powered-lift acoustic testing with appropriate wing and flap segments.

The emphasis in this paper is on the overall acoustic performance of the QCSEE UTW powered-lift system. Although the test data obtained provide a basis for analysis of both full-scale jet-flap noise and engine noise reflection for the engine, wing and flap geometries used, these efforts are beyond the scope of this paper. The evaluation of a bulk absorber treatment for the QCSEE UTW fan exhaust is reported in Ref. 10.

ENGINE AND WING CONFIGURATIONS

A variety of engine and wing configurations were tested in the NASA UTW engine test program. In addition to the fully suppressed engine configuration (Fig. 1), the engine was tested in the powered-lift mode with the fan exhaust acoustic splitter and core exhaust treatment removed. Because of cost, weight, and complexity associated with the fan exhaust duct acoustic splitter and the stacked core noise treatment, the acoustic performance without these elements would be of interest in relation to designing treatment to meet a less severe application, such as a 914.4-meter (3000-ft) runway aircraft. A completely hardwall version with a bellmouth inlet was also tested for baseline (unsuppressed) acoustic performance. The wing-flap segment used was a modified 2-flap NASA supercritical airfoil design recommended by NASA Langley for short-haul aircraft as described in Ref. 11. The location of the engine relative to the wing-flap system was based on Langley data. The configuration gives good powered-lift performance. No consideration was given, however, to acoustic optimization. Wing-flap configurations included four different settings of the flap trailing edge angle ψ, as shown in Fig. 4. Two takeoff settings with $\psi = 20^{o}$ and $\psi = 30^{o}$, an approach setting with $\psi = 60^{o}$, and a fully retracted "cruise" position were tested. The flap angles are measured from the main wing segment chord centerline to the flap chord centerline. Dimensions of the engine and the wing and flap cross-sections are also shown in Fig. 4. The separation distance ratio (X/D) was typically about 5 in takeoff and 4 in approach, where X is the distance from the fan exhaust exit plane to the engine centerline intersection with the flap, as shown in Fig. 4, and D is the engine fan exhaust diameter. The engine centerline was 4.57 meters (15 ft) above

ground level. The span of the wing-flap system was 7.31 meters (24 ft) with the upper edge 7.92 meters (26 ft) above ground level.

The variable-pitch fan of the UTW engine provided a capability of achieving approach thrust in two different ways: operating at takeoff fan blade angle and at lower fan speed, or operating at takeoff fan speed and at a lower fan blade pitch angle (flatter fan pitch). The latter configuration was preferred because it allows a quicker conversion from approach to takeoff thrust (shorter approach to forward thrust transient time), and is the configuration used for UTW approach acoustic data in this paper. Engine-alone tests indicated that perceived noise level was rather insensitive to fan blade angle for a given engine thrust.[12] The variable geometry UTW fan exhaust nozzle also permitted an increase in nozzle area at approach to obtain approach thrust with a lower effective engine exhaust velocity and a higher engine weight flow.

TEST FACILITY AND INSTRUMENTATION

The QCSEE engines were tested in the NASA-Lewis Engine Noise Test Facility (Fig. 5). Each engine was tested alone and also with appropriate unswept wing and flap segments properly located to simulate the powered-lift system of an aircraft in flight. Wing and flaps were mounted with spans vertical to minimize flow field ground interference. A photograph of the facility is presented in Fig. 6.

Two microphone systems were employed in the test program, a ground plane system, and an overhead system. The 14 ground microphones were positioned at 10° increments at selected locations on a 45.7-meter (150-ft) radius arc. Microphones located within 10° or 20° of the deflected jet flow line, during the engine and wing tests, were severely buffeted and were moved to other locations outside the flow stream for these tests. These ground plane microphones provided flyover plane noise data, that is, for the case in which the aircraft flies directly over an observer on the ground. The flyover plane is shown in Fig. 7 as the plane AA'B'B. The angle θ_F is measured from the flight path AA' to the line O_FP defined by the position of the flyover observer at point O_F and the aircraft at point P. The QCSEE inflight noise goals, however, are specified for a 152-meter (500-ft) sideline flyby, as shown in Fig. 3. The sideline plane is the plane AA'C'C in Fig. 7. The angle θ_S is measured in the sideline plane from AA' to the line O_SP defined by the sideline observer at O_S and the aircraft at P. To obtain sideline noise data, five microphones were hung from a cable suspended from two towers, all lying in a plane 90° to the engine axis, as shown in Figs. 5 and 6. The microphones were spaced to provide proper angles relative to a ground observer for an aircraft at altitudes of 0, 30.5, 61.0, 91.4, and 122 meters (0, 100, 200, 300, and 400 ft). A sixth microphone was located to represent an observer at 120° from the engine inlet with the aircraft at 61.0 meters (200 ft) by use of a portable boom or a second cable from the main tower to a ground support point. Preliminary studies had indicated 61.0 meters (200 ft) to be the altitude of maximum sideline flyby noise.[5] In this paper data obtained by the ground plane microphones relate to the flyover plane, and those obtained by the overhead microphones relate to the sideline flyby geometry.

Bruel and Kjaer 1.27-centimeter (0.5-in.) diameter condenser microphones equipped with windscreens were used. The ground plane microphones were secured to 1.2 by 1.2 meters (4 by 4 ft) hard boards with microphones pointed nominally toward the noise source. The paved asphalt test area surface was painted white, except for the region within 15.2 meters (50 ft) of the engine center, to minimize acoustic distortions due to convected heat waves rising from the black asphalt surface.

The data acquisition system utilized a minicomputer to control the noise and aerodynamic data scanners. Noise data from each microphone were analyzed on-line by an automated 1/3 octave band spectrum analyzer. Sound pressure level spectra (referenced to 2×10^{-5} N/m^2) were determined for each microphone over the frequency range from 25 Hz to 16 kHz. The digitized noise data were transmitted to the computer. Each of three samples for a given corrected fan speed was reduced separately. The arithmetic average was then adjusted to standard acoustic day atmospheric conditions (77^{0} F, 70 percent RH). The analog noise data were also recorded on FM tape for later off-line data reduction. Aerodynamic and environmental data were sampled periodically during the noise data acquisition scan and also transmitted to the computer. These data included engine fan and core speeds, fuel flow, engine pressures and temperatures, engine thrust, wind speed and direction, ambient and dew-point temperatures and barometric pressure. Data from the multiple aerodynamic and environmental scans were averaged and used by the computer in the calculation of engine operating parameters. At the conclusion of the test point, the noise data and calculated engine operating parameters were outputted on a line printer. Data stored in the computer were transmitted on command to the Central Data Collector for storage and detailed analysis.

Perceived noise levels (PNL's) on a 152-meter (500-ft) sideline flyby with the aircraft at different specified altitudes were calculated using data from the overhead microphone system. From these PNL values effective perceived noise levels (EPNL's) were also calculated. These calculations were made as specified in "Inflight and Reverse Thrust Noise Calculation Procedure" (Appendix A, Vol. II, Ref. 4). The procedure accounts for a number of effects, including atmospheric attenuation, extra ground attenuation, fuselage shielding, inlet flow cleanup during flight, relative velocity, and OTW wing shielding.

The measured ground plane microphone data were corrected to free field by application of a -6-dB correction to each 1/3 O.B. SPL value. For the overhead microphones a nominal -2-dB free-field correction was determined from both analytical and empirical studies. The ground reflection characteristics of each of the overhead microphones was unique, and a spectral correction for each was empirically determined and applied in cases where precise absolute values were desired or where comparisons between overhead microphones were to be made.

Although it is desirable to measure far-field acoustic data at a distance of some 50 source diameters or characteristic lengths if possible, the interpretation of acoustic data obtained for large distributed sources in a limited test area where this criteria cannot be met requires some caution. In the engine-alone case the ground plane microphones were at a nominal 24 engine exhaust diameters (1.9 m (75 in.)) from the source, the overhead

microphones at 90° from the engine are typically some 25.3 meters (83 ft) or about 13 diameters away, and the 120°/61-meter (200-ft) overhead microphone at about 17.7 meters (58 ft) is only 9.3 diameters away from the source. However, in the powered-lift mode the high end of the trailing edge flap is a principal noise source location, and is relatively close to the microphones of the overhead system. The overhead microphones at 90° from the inlet are nominally 24.4 meters (80 ft) from this flap edge. Furthermore, the 120°/61-meter (200-ft) microphone of the overhead system is less than 12.8 meters (42 ft) from the high end of the flap trailing edge. This edge is typically 12.7 meters (41.7 ft) from the engine inlet, and if this distance is indeed a characteristic length of the powered-lift source, the overhead microphones are only 1 or 2 such lengths away.

Because of the questionable microphone and source geometry, anechoic chamber tests were conducted using a 1/17 scale model of the QCSEE UTW wing and flap configuration to determine deviations from the far-field noise associated with "close-in" measurement of jet-flap interaction noise. "Close-in" through far-field data were obtained in the flyover plane at radiation angles θ_F of 90° and 120° from the engine inlet (see Fig. 7). In addition, similar tests were run at radiation angles θ_S of 90° and 120° simulating the 61-meter (200-ft) altitude sideline condition (ϕ of 68°) with the simulated ground plane in position.

These tests indicated very little error in the flyover plane microphone data (ϕ = 0°) at θ_F of 90° from the engine inlet with either takeoff or approch flaps. However, the θ_F = 120° microphone jet-flap close-in noise spectrum was 3.9 PNdB higher than the far-field microphone spectrum for the takeoff flap configuration, and 1.5 PNdB for the approach flap configuration. No near-field adjustments were made to the ground plane (ϕ of 0°) microphone data, however, because these microphones were used only to establish approximate directivity patterns in the flyover plane (varying θ_F), and appropriate corrections for θ_F values other than 90° and 120° were unavailable.

Absolute values are required, however, for the sideline flyby microphone system. Small spectral corrections were determined and applied for the low-frequency jet-flap noise portion of the θ_S of 90°/61-meter (200-ft) sideline (ϕ of 68.2°) microphone spectrum with approach flaps. Conversely, no correction was indicated for the takeoff flap configuration. At θ_S of 120°/61 meters (200 ft) (ϕ of 68.2°) in the sideline plane, however, a very large correction of more than 7 PNdB was required for the jet-flap noise with approach flaps and about 5 PNdB with takeoff flaps.

Since the measured spectrum at the θ_S of 120°/61-meter (200-ft) (ϕ of 68.2°) sideline microphone is a combination of widely distributed jet-flap noise and engine noise from a distant source, the complexity of the problem forbids a simple corrective procedure. It was decided, therefore, to avoid use of the θ_S of 120°/61-meter (200-ft) microphone data because of the unacceptably large uncertainty of the data. The calculation of an EPNL value in accordance with the procedure of Ref. 4 normally requires a maximum forward and a maximum aft PNL value. Consequently, the necessary maximum forward and aft PNL values were constructed from the measured θ_S = 90° sideline flyby microphone data and relative values determined from measured engine-alone noise and the best available jet-flap noise predic-

tions.[13,14,15] Thus, the EPNL values are based entirely on the sideline flyby overhead microphones at θ_S of 90° from the engine inlet.

TEST RESULTS

Jet-Flap Noise

Analysis of the UTW engine powered-lift test data indicated that the altitude of maximum sideline flyby noise was 91.4 meters (300 ft) for both takeoff and approach conditions. This is the most significant direction with respect to the QCSEE noise goals. In Fig. 8 measured and predicted powered-lift system noise spectra are compared at this maximum noise altitude for takeoff conditions with a 30° flap setting. The NASA 1973 jet-flap noise prediction[13] (dashed line in the figure) peaks at a very low frequency and falls off rapidly at the higher frequencies. The measured engine-alone noise (circles) is well below the jet-flap noise in the low frequency jet noise region but exceeds the jet-flap noise at the mid and high frequencies. The antilogarithmic addition of the corresponding SPL values of these two sources yields the predicted spectrum for the powered--lift system (solid line in the figure). It can be seen in the figure that the predicted powered-lift spectra in the region below 160 Hz is primarily controlled by jet-flap noise, while the higher frequencies are controlled by engine-alone noise. The jet-flap prediction and the engine-alone noise are at approximately the same PNL level, 90.8 and 91.0, respectively, presenting a balanced condition in which neither source dominates the overall PNL.

The measured powered-lift spectrum (squares) is in excellent agreement with the predicted curve in the low-frequency region where the SPL levels are essentially due to jet-flap noise, indicating excellent agreement with the NASA 1973 jet-flap noise prediction. However, at the higher frequencies above 200 Hz where the SPL levels are controlled primarily by engine noise, these levels are 5 to 7 dB higher than the engine-alone noise at nearly all frequencies up to 10 kHz rather than the sum of the jet-flap noise prediction and engine-alone noise levels.

The most likely explanation of the increase in powered-lift system engine noise levels relative to engine-alone noise levels appears to be the reflection of engine noise into the microphones from the wing and flap surfaces. The result is an increase of nearly 4 dB in PNL of the poweredlift system noise at takeoff conditions as indicated in the figure.

The situation at approach conditions with a 60° flap setting is much the same. Again the low-frequency jet-flap noise shows good agreement between the measured and predicted levels, as shown in Fig. 9. Here again, the measured system spectra at the higher frequencies shows a 4- to 8-dB broadband noise increase over predicted values. In particular, the 920-Hz blade passing frequency tone is 9 dB over the expected level. The assumed reflection phenomenon results in an increase of 3.5 dB in the PNL of the fully suppressed engine at approach conditions.

A comparison of measured and predicred powered-lift noise at the 90° flyover direction (ϕ = 0°, θ_F = 90°, Fig. 7) is of particular interest for two reasons. First, the jet-flap noise descriptions and prediction models[13,14,15] usually are referenced to this direction. Second, since

the acoustic reflection characteristics between the QCSEE overhead and ground microphone systems differ greatly, the 90° flyover acoustic data provide a further check on the apparent engine exhaust noise reflection exhibited in the preceding two figures.

Measured and predicted powered-lift spectra for the fully suppressed UTW engine at takeoff conditions in the flyover plane are compared in Fig. 10. As in the two previous figures, the NASA 1973 jet-flap noise prediction is represented by the dashed line and the measured engine-alone noise by circles. The combination of the two yields a prediction of the total system, or the powered-lift noise, shown by the solid line. Here again, at the low-frequency end of the spectrum where the predicted curve is essentially due to jet-flap noise only, the measured data shown by the squares is in excellent agreement. At higher frequencies, above 200 Hz, the measured spectra generally lies above the predicted, but periodic peaks and valleys appear, and the measured spectrum may be as much as 10 dB above (at 1000 Hz) or as much as 3 dB below (at 2000 Hz) the predicted spectrum. Possible reflection reinforcements appear at 200, 1000, and 4000 Hz, with possible cancellations at 400, 2500, and 1000 Hz. The measured powered-lift PNL is 3 dB above the predicted curve as a result of the apparent reflection phenomenon.

Similar data are plotted in Fig. 11 for approach conditions. Agreement of the measured data with the predicted powered-lift spectrum is only fair at the low frequencies. At higher frequencies the measured powered-lift spectra behaves somewhat as in the takeoff case. Possible reinforcement peaks occur at 1000 and 3150 Hz, and possible cancellations appear at 630 and 2000 Hz. The measured powered-lift PNL exceeds the predicted by only 0.4 dB.

Similar results were obtained in a powered-lift noise experiment with a highly suppressed TF 34 engine with a wing and flap system.[16] A 4- to 5 PNdB noise increase was attributed to a redirection and reflection of the engine exhaust noise by the wing-flap system. The data were measured in the flyover plane.

Flap Position

The effect of the wing and flap system on the noise output of the fully suppressed UTW engine at takeoff power is shown in Fig., 12. The addition of the wing with cruise flaps (see Fig. 4) results in a 3- to 5-dB increase in PNL in the region of 50° to 110° in the flyover plane (Fig. 12(a)). Progressively larger increases are noted for the 30° and 60° flap settings. Data at 110° through 140° for the 60° flap configuration were not obtainable because of flow impingement on the microphones due to the deflected jet as noted previously in the instrumentation section. The data indicate that, except for the 60° flap position, the flyover plane PNL values are dominant in the aft quadrant at 120° from the inlet where engine noise dominates the noise field.

Sideline flyby powered-lift noise data at 90° from the inlet (Fig. 12(b)) show a decided increase in sideline noise with increase in aircraft altitude up to about 91.4 meters (300 ft), the "maximum sideline noise altitude," followed by a reduction in noise with further increase in altitude.

The "maximum sideline noise altitude" is the end product of a number of independent factors. At low aircraft altitudes (ϕ values near 90^0) the short slant distance from the aircraft to the observer (line POs in Fig. 7) results in higher noise levels than at higher altitudes. However, UTW jet-flap noise is strongest near the flyover plane (ϕ values near 0^0). The combination of these two factors results in a maximum at some intermediate altitude between the extremes. Differences in signal reflection effectiveness for different ϕ angles for a given engine-wing-flap geometry combination also influence the location of the maximum noise altitude. A fourth factor is extra ground attenuation (EGA). Since this attenuation was applied to that portion of the slant distance lying within the assumed turbulent boundary layer of the earth, 30.4 meters (100 ft), the effect of EGA is to shift the maximum noise location to higher altitudes. EGA was included in the EPNL calculations but not in PNL calculations.

For a purely axisymmetric source a monotonic falloff of sound level with increasing altitude is to be expected, as indicated approximately by the engine-alone noise of Fig. 12(b) (and somewhat more precisely by the engine-alone noise of Fig. 13(b)).

At engine approch power the flyover plane (Fig. 13(a)) engine-alone noise in the forward quadrant between θ_F of 0^0 and 80^0 is higher than for the takeoff power case due to the lack of high throat Mach number inlet suppression at approach power, while the aft radiated sound level is lower due to the reduced engine pressure ratio and exhaust velocities. As in the previous case, there is an increase in PNL at a flap angle of 30^0; however, a reduction occurred at 60^0. Both engine and jet-flap noise fall off rapidly for θ_F greater than 140^0.

In the sideline flyby (Fig. 13(b)), the PNL variation with altitude is similar to that at takeoff, with maximum PNL values occurring at about 91.4 meters (300 ft) altitude when the wing and flaps are in place. The falloff of PNL with increase in altitude for the engine-alone noise is consistent with the increase in slant distance for an axisymmetric source, as previously noted.

The effect of flap angle on powered-lift noise is shown in Fig. 14 for both takeoff and approach power. PNL variations with change in flap angle, ψ, are plotted for three selected microphone directions. The UTW powered-lift system noise increased on the order of 1 PNdB per 10^0 change in flap angle at takeoff power (Fig. 14(a)) for the 91.4-meter (300-ft) sideline flyby direction and also the 90^0 flyover direction, and about 1 PNdB per 7.5^0 flap angle increase at the 30^0 flyover direction. At approach power, (Fig. 14(b)), the system PNL at the 60^0 flap angle showed no significant increase over the cruise flap configuration. PNL values at the 20^0 and 30^0 flap angles are 1 to 4 dB higher than those at the extreme settings, while in the sideline flyby plane they increased on the order of 1 dB per 25^0 increase in flap angle. An OASPL variation of about 1 dB per 7^0 change in flap angle was reported in Refs. 13 and 14 for jet-flap noise only in the flyover plane. Thus, at takeoff power the total system PNL is rather sensitive to the flap angle, which may be interpreted as a strong indication that the jet-flap noise is the dominant contributor to the total system noise. However, as indicated in the following discussion, the wing and flap reflection of the engine noise is the far more likely explanation

for the apparent sensitivity to flap trailing-edge angle. At approach power the effect of the flap angle is negligible, and the system appears to be dominated by engine noise.

The spectral variation for the different flap angles is given in Fig. 15 for the sideline flyby 91.4 meters (300 ft) altitude microphone direction at takeoff power. The low-frequency jet noise for the fully suppressed engine-alone case is very low, and the increase in the low-frequency noise at increased flap angle is consistent with jet-flap noise generation. However, at the mid and high frequencies, 500 Hz and higher, a pronounced increase is observed due to the presence of the cruise flap, followed by only slight increases due to the increase in flap angle associated with the 30^{o} and 60^{o} flap configurations. Here again, the 4- to 11-dB increase in SPL values in the mid and high frequencies is consistent with fan exhaust noise reflection from the wing and flap surfaces. If this is the case, it appears that positioning of the first and second flaps to more nearly face the engine and microphone (see Fig. 4) results in a further increase in reflected signal strength as indicated by the 30^{o} and 60^{o} flap data.

Exhaust Velocity

The variation of PNL with engine exhaust velocity (ideal mass weighted fan and core) for the takeoff ($\psi = 30^{o}$) and approach ($\psi = 60^{o}$) flap configurations is shown in Fig. 16 for the fully suppressed engine. All the data points were obtained at the takeoff fan blade angle and the same fan exhaust nozzle area. Previous jet-flap interaction noise experiments indicate an OASPL variation with the 6.7 power of the engine exhaust velocity.[14] Jet-flap noise includes both quadrapole and dipole sources with eighth and sixth power variations with velocity, respectively. For the engine noise components a sixth power or lower OASPL variation would be expected. However, PNL values have low sensitivity at the low frequencies where the UTW jet-flap noise peaks. Furthermore, the enhancement of engine noise by reflection would further increase the expectancy of lower exponents than the sixth power.

As shown in Fig. 16(a) with a 30^{o} flap setting a PNL variation with the 5.7 power was obtained at the 90^{o}/91-meter (300-ft) sideline flyby direction. In the flyover plane the 30^{o} direction showed the effect of the hybrid inlet which gives increased suppression with increased engine airflow. The effect is also noted, but to a lesser degree, at the 90^{o} flyover direction. At the 120^{o} flyover direction, the 6.8-power variation suggests some quadrapole radiation in this direction.

With a 60^{o} flap setting (Fig. 16(b)) a PNL variation with the 6.7 power was observed for the 90^{o} sideline flyby direction, and also for the 90^{o} flyover direction. At 150^{o} in the flyover direction, the velocity exponent was only 5.8. The 30^{o} flyover direction again shows the influence of the hybrid inlet with a reduction in velocity exponent with increased engine power and inlet airflow.

The powered-lift system noise data here represent a combination of quite different noise sources, and a rather detailed knowledge of their content would be required to fully explain the velocity exponents obtained.

Hybrid Inlet

The suppression provided by the hybrtid inlet is illustrated in Fig. 17 for the fully suppressed engine. As engine airflow increases through the throat section of the inlet the average one-dimensional throat Mach number approaches the takeoff design value of 0.79. The acoustic radiation from the inlet must travel forward against the high velocity inlet flow and is attenuated by this version of the "sonic inlet" concept. The circles represent the spectra at approach power conditions with a prominent blade passing frequency tone visible at 800 Hz. With an increase in engine power to takeoff power, the low-frequency jet-flap noise is increased by typically about 4 dB. However, as the inlet Mach number increases from 0.60 to 0.79, the tone disappears and the fan broadband noise at higher frequencies is reduced by as much as 14 dB. And although the thrust increased by 30 percent, the PNL was reduced by 4.3 PNdB.

Reduced Aft Suppression

In the QCSEE program 914 meters (3000 ft) runway versions of the QCSEE engines were studied. With the 305-meter (1000-ft) longer runway smaller engines and faster takeoff and approach speeds result in a lower powered-lift EPNL noise level. Such an engine, then, with reduced acoustic suppression, could still be acoustically competitive with the prime 610-meter (2000-ft) runway aircraft engine.

The elimination of the fan exhaust duct acoustic splitter and the stacked core noise treatment would result in a simpler, lighter, and lower drag engine for a given engine design thrust. Consequently, the QCSEE UTW engine was tested with the fan exhaust duct splitter and the stacked core noise treatment removed.

PNL values for the reduced aft suppression configuration are compared with the fully suppressed data for the flyover case in Fig. 18(a) and the sideline flyby case in Fig., 18(b). Removal of the fan exhaust duct acoustic splitter and the core exhaust noise treatment resulted in an increase in sideline flyby noise of about 4 dB at the maximum noise altitude direction (91.4 m (300 ft)) for takeoff conditions, as shown in Fig. 18(b). This effect, due to differences in radiated aft end noise, was progressively weaker at directions closer to the inlet direction, as indicated in the flyover plane data of Fig. 18(a).

The effectiveness of the complete acoustic suppression system is indicated by the difference in PNL for the fully suppressed engine and the hardwall baseline case, as also shown in Figs. 18(a) and (b). The sideline flyby perceived noise levels for the fully suppressed engine are 7 to 9 dB lower than the baseline in Fig. 18(b), a level of suppression comparable to that previously obtained in engine-alone acoustic tests. Part of this difference, but not more than 1 dB, may be attributed to the higher flap angle (30^{o}) for the hardwall baseline case relative to the 20^{o} angle for the other two configurations.

In Fig. 19 the spectra for the three configurations at takeoff conditions are presented for a sideline flyby at 91 meters (300 ft) altitude. The differences at low frequency are rather minor, since this is the region

of jet-flap noise dominance which is relatively unaffected by changes in suppression. Above 500 Hz the higher spectral levels are primarily due to fan exhaust noise. In this region the reduced aft suppression configuration results in an SPL increase of 2.5 to 8 dB over the fully suppressed configuration, while the hardwall baseline produces a further increase with individual SPL values some 5 to 15 dB above the fully suppressed levels.

The BPF tone is visible in the baseline spectrum. The 4-dB increase in PNL associated with the reduced aft suppression configuration resulted from an apparent increase in combustor noise (with peak frequency of 400 Hz) and an increase in fan exhaust broadband noise in the region above 800 Hz.

Since a significant reduction in engine exhaust noise is a prime requirement for attainment of the 95-EPNdB noise goal by the UTW powered-lift system, the reduced aft suppression configuration would probably be attractive only for a less severe noise goal.

INFLIGHT NOISE LEVELS

Calculated UTW inflight noise levels are plotted in Fig. 20 for the fully suppressed and reduced aft suppression configurations at takeoff and approach conditions. At takeoff the maximum EPNL value for the fully suppressed engine was 99.7 EPNdB at 91.4 meters (300 ft) altitude, 4.7 dB over the goal (Fig. 3). At approach the maximum of 98.5 EPNdB also occurred at 91.4 meters (300 ft) altitude and was 3.5 dB over the goal. With reduced aft suppression the maximum takeoff level was 103.9 EPNdB, and the maximum approach level was 100.9 EPNdB.

Although the QCSEE UTW powered-slift system noise exceeded the very stringent 95-EPNdB noise goal, the UTW engine represents a significant advance in low noise jet engine technology. A four-engine QCSEE UTW powered-lift aircraft would be 14, 7, and 13 dB, respectively, below the very strict FAA FAR 36 1978 Stage 3 noise limits at the takeoff, approach, and sideline noise measuring locations.

The inflight noise levels higher than the goal are apparently due to three factors. First, at the inception of the QCSEE program in early 1974, a reduction of 3.5 dB was applied to the UTW jet-flap noise prediction of Ref. 13 to provide a baseline for determining fan pressure ratio and exhaust velocities for the QCSEE UTW engine. The intent was to anticipate the availability of a lower noise advanced design flap for the time period at which short-haul powered-lift systems saw commercial appalication, and to avaoid penalizing the engine with an unnecessarily low-pressure ratio and consequent higher engine fuel consumption, drag, and weight. However, the UTW engine was tested with a 1974 state-of-the-art wing-flap design rather than with an advanced design.

Second, static ground testing of the engine alone at the General Electric Peebles Fest Facility[12] indicated that forward and aft maximum PNL values were on the order of 4 and 3 dB higher, respectively, than the design values. At approach the corresponding values were 3.5 and 5 dB, respectively, higher than design.

And third, the measured powered-lift system takeoff and approach PNL values at the maximum noise altitude were 3.9 and 3.5 dB, respectively, higher than predicted in Figs. 8 and 9 due to unaccounted for reflection of fan exhaust and engine core noise. Thus, the 99.7-EPNdB inflight noise value at takeoff (Table 2) is consistent with the increases in engine noise, jet-flap noise, and reflected engine noise relative to the design value of 93.6 EPNdB.[8]

Likewise, at approach the inflight noise level of 98.5 EPNdB (Table 2) is consistent with the increases in measured levels relative to the design level of 93.6 EPNdB.[8]

On the basis of these tests a balanced acoustic design between jet-flap noise and engine noise must make allowance for the reflection effects of engine noise due to the presence of the wing-flap system. This requires that the engine noise plus its amplification due to reflection have approximately the same PNL value as the jet-flap noise component.

The ability of the QCSEE UTW powered-lift system to meet the 95-EPNdB noise goal would be benefitted by improvements in three different areas: (1) a reduction in engine exhaust noise; (2) a reduction in engine noise reflected from the wing-flap system to the sideline flyby microphone system; and (3) a reduction in UTW jet-flap interaction noise. There is a potential for achieving reductions in these three areas.

The variable-pitch fan requirement for the UTW engine to provide a capability to rotate the fan blades in either direction through flat pitch or feather to reach the reverse thrust orientation favored a low solidity, composite blade, small blade number, and low tip-speed fan design. This design represented a departure from the more conventional fan design family for which acoustic design experience and verified correlation models exist. Lower noise levels for this type fan may be expected as additional design experience and research efforts are applied.

The orientation of the wing-flap system relative to the engine was not considered in relation to minimizing acoustic reflection in the directions of major importance to a specified noise goal. Research effort in this area may allow significant reductions of the reflection levels encountered in the UTW engine-wing tests, perhaps by the use of a swept wing rather than an unswept one, and by relocation of the engine relative to the wing and flaps.

A number of concepts have been investigated by experimenters in attempts to significantly reduce UTW jet-flap interaction noise. McKinzie[17] has obtained a reduction of 6 and 5 dB at takeoff conditions over a wide range of radiation angles in the flyover and sideline planes, respectively, with a 1/17 scale model of the QCSEE UTW wing-flap system. The improvement was attributed to the alteration and subsequent reduction of three dominant noise sources by the use of short spanwise faired plugs, centered in relationship to the nozzle axis, in the slots between the wing and flaps of the configuration.

At approach a 5-dB reduction was obtained in the forward quadrant in the flyover plane with no improvement in the sideline plane. Only small

reductions were noted in the flow-turning efficiencies and turning angles due to the plugs.

COMPARISON OF UTW AND OTW POWERED-LIFT ACOUSTIC PERFORMANCE

The UTW and OTW powered-lift system acoustic performance values are compared in Table 2. At takeoff the UTW system is 1.3 dB higher than the OTW system. At approach the UTW is about 4 dB above the OTW system. The UTW takeoff and approach average is 99.1 EPNDB, 4 dB over the 95 EPNdB goal, while the OTW average is 96.5, only 1.5 dB over the goal. The 95-EPNdB contour area of the UTW system is 1.0 square mile (2.6 km^2); the OTW system contour area is 0.5 square mile (1.3 km^2). Although the OTW system meets the goal, the UTW is over the goal.

For comparison purposes the noise contour areas of the QCSEE-powered aircraft are shown in relation to that of a typical wide body aircraft in Fig. 21. It can be seen that the UTW area is only about one-third that of the DC-10 and therefore represents a significant improvement over the wide body aircraft. Even greater advantages are noted for the OTW contour area.

A "head-to-head" comparisons of the UTW and OTW powered-lift system spectra is presented in Fig. 22 at the maximum sideline noise altitude for both takeoff and approach conditions. No adjustment in acoustic levels was made for the slightly higher thrust of the OTW engine. At the 152-meter (500-ft) sideline 91.4 meters (300 ft) altitude direction the UTW system PNL of 98.7 PNdB is 0.5 PNdB higher than the OTW PNL at takeoff (Fig. 22(a)). Although the UTW low-frequency jet-flap sound level is lower than that produced by the OTW at takeoff, the radiated and reflected engine noise in the mid and high frequencies exceeds that of the OTW system. It appears that the latter difference is largely due to the wing shielding of the engine noise, an advantage of the OTW system. A similar effect occurs in the approach case (Fig. 22(b)) where the difference is 2.6 PNdB.

The effect of wing shielding or wing reflection on the noise spectra for the OTW or UTW configurations, respectively, at takeoff conditions is presented in Fig. 23. As shown in Fig. 23(a) although the wing-flap system of the OTW configuration presented an additional noise source, that is, jet-flap noise, there was a reduction of about 5 dB in the portion of the spectrum above 900 Hz due to wing shielding of the fan exhaust and core noise. Although there was a significant increase at low frequencies where the jet-flap noise is dominant, the net result was a PNL reduction of 2.8 dB below the engine-alone case. In the UTW system the addition of the wing resulted in an increase of noise level throughout the spectrum, as shown in Fig., 23(b), and a PNL increase of 7 dB over the engine-alone case. Although the UTW engine-alone noise was 8.7 dB below that of the OTW engine, in the powered-lift mode the UTW system perceived noise level was 0.9 dB higher. Furthermore, the OTW powered-lift thrust was 10 percent greater. Thus, because of the wing shielding advantage of the OTW system, the UTW engine-alone noise level must be somewhat lower than the OTW engine noise to meet the same powered-lift noise specification.

SUMMARY AND CONCLUSIONS

The measured powered-lift data were in reasonably good agreement with earlier tests of UTW engine noise and experimental studies of jet-flap noise. The hybrid inlet performed well. At takeoff and approach the UTW powered-lift system perceived noise levels were dominated by reflected engine noise. Spectrally, the jet-flap noise was dominant at very low frequencies while reflected engine noise was dominant at the mid and high frequencies. The reflection of engine noise from the UTW unswept wing and flap system produced an unaccounted for 3- or 4-dB increase in inflight noise levels. A reduced aft suppression configuration gave inflight noise levels that were 4.2 dB higher at takeoff and 2.4 dB higher at approach than the fully suppressed engine configuration levels.

The UTW takeoff noise level was about 4.7 dB higher than the goal while the approach value was 3.5 dB over the 95-EPNdB goal. However, the UTW configuration is still considerably quieter than the current low-noise wide body jet transports. The UTW system noise was about 1.3 dB higher than the OTW system at takeoff, and about 4 dB higher at approach. The UTW 95 EPNL noise contour area of 2.6 square kilometers (1.0 mi^2) is well above the 1.3 square kilometers (0.5 mi^2) of the OTW system which just meets the noise goals, but is only about one/third that of the DC 10-10 quiet wide body jet transport.

The engine-alone PNL at the maximum noise sideline flyby direction was increased by 7 dB by the addition of the unswept wing-flap system at takeoff conditions. However, for the OTW system the presence of the wing-flap system resulted in a reduction of 2.8 dB below the engine-alone noise. For equal powered-lift system total noise the UTW engine-alone noise must be somewhat lower than that of the OTW engine-alone noise. This means that the OTW engine can use a higher fan pressure ratio and a higher fan tip speed to provide a smaller and lighter engine to achieve the same thrust and powered-lift noise level as a corresponding UTW engine installation.

REFERENCES

1. Ciepluch, C. C., "A Review of the QCSEE Program," NASA TM X-71818, 1975.

2. Ciepluch, C. C., "Overview of the QCSEE Program," Powered-Lift Aerodynamics and Acoustics Conference, NASA SP-406, 1976, pp. 325-333.

3. Loeffler, I. J., "QCSEE Engine and Wing Tests at NASA," Quiet, Powered-Lift Propulsion Conference, NAS 2077, 1979, pp. 249-261.

4. Loeffler, I. J., Smith, E. B., and Sowers, H. D., "Acoustic Design of the QCSEE Propulsion Systems," Powered-Lift Aerodynamics and Acoustics Conference, NASA SP-406, 1976, pp. 335-356.

5. "Quiet Clean Short-Haul Experimental Engine (QCSEE) - Preliminary Analyses and Design Report," NASA CR-134838-VOL-1 and NASA CR-134839-VOL-2, 1974.

6. "Quiet Clean Short-Haul Experimental Engine (QCSEE) - Under-the-Wing (UTW)," NASA CR-134847, 1977.

7. "Quiet Clean Short-Haul Experimental Engine (QCSEE) - Over-the-Wing (OTW) Design Report," NASA CR-134848, 1977.

8. Sowers, H. D., and Coward, W. E., "Quiet Clean Short-Haul Experimental Engine (QCSEE) - Under-the-Wing (UTW) Engine Acoustic Design," NASA CR-135267, 1978.

9. Sowers, H. D., and Coward, W. E.: "Quiet Clean Short-Haul Experimental Engine (QCSEE) - Over-the-Wing (OTW) Engine Acoustic Design," NASA CR-135268, 1978.

10. Bloomer, H. E., and Samanich, N. E., "QCSEE Fan Exhaust Bulk Absorber Treatment Evaluation," AIAA Paper 80-0987, June 1980. Also NASA TM-81498.

11. Whitcomb, R. T., "Review of NASA Supercritical Airfoils," ICAS Paper 74-10, Aug. 1974.

12. Stimpert, D. L., "Quiet Clean Short-Haul Experimental Engine (QCSEE) - Under-the-Wing (UTW) Composite Nacelle Test Report, Vol. II - Acoustic Performance," NASA CR-159472, 1979.

13. Clark, B. J., Dorsch, R. G., and Reshotko, M., "Flap Noise Prediction Method for a Powered-Lift System," AIAA Paper 73-1028, Oct. 1973.

14. Dorsch, R. G., Clark, B. J., and Reshotko, M., "Interim Prediction Method for Externally Blown Flap Noise," NASA TM X-71768, 1975.

15. Fink, M. R., "A Method for Calculating Externally Blown Flap Noise," NASA CR-2954, 1978.

16. Samanich, N. E., Heidelberg, L. J., and Jones, W. L., "Effect of Exhaust Nozzle Configuration on Aerodynamic and Acoustic Performance of an Externally Blown Flap System with a Quiet 6:1 Bypass Ratio Engine," AIAA Paper 73-1217, Nov. 1973. Also NASA TM X-71466.

17. McKinzie, D. J., Jr., "Measured and Prediction Impingement Noise for a Model-Scale Under-the-Wing Externally Blown Flap Configuratuion with a QCSEE-Type Nozzle," NASA TM-81494, 1980.

TABLE 1. - ACOUSTIC DESIGN PARAMETERS

	UTW engine	OTW engine
Fan diameter, cm (in.)	180.4 (71)	180.4 (71)
Number of fan blades	18	28
Number of stator vanes	33 (32 + pylon)	33 (32 + pylon)
Vane/blade ratio	1.83	1.18
Inlet treatment length/fan diameter (L/D)	0.74	0.74
Rotor/stator spacing, rotor tip chords	1.5	1.93
Takeoff conditions		
Fan speed (rpm)	3089	3738
Fan tip speed, m/sec (ft/sec)	289.6 (950)	350.5 (1150)
Fan pressure ratio	1.27	1.34
Fan weight flow (corr), kg/sec (lbm/sec)	405.5 (894)	405.5 (894)
Core weight flow (corr), kg/sec (lbm/sec)	31.3 (69.1)	35.7 (78.6)
Fan exhaust area, m^2 (in^2)	1.615 (2504)	{1.802 (2794)
Core exhaust area, m^2 (in^2)	0.348 (540)	(total area)}
Fan exhaust velocity, m/sec (ft/sec)	197.8 (649)	219 (720)
Core exhaust velocity, m/sec (ft/sec)	238.9 (784)	328 (1077)
Bypass ratio	12.1	10.3
Uninstalled thrust, SLS, kN (lbf)	81.39 (18,300)	93.4 (21,000)
Installed thrust, SLS, kN (lbf)	77.4 (17,400)	90.3 (20,300)
Fan blade passing frequency, Hz	920	1744
Aircraft speed, m/sec (knots)	41.2 (80)	41.2 (80)
Approach conditions		
Fan exhaust area, m^2 (in^2)	1.615 (2504)	{1.802 (2794)
Core exhaust area, m^2 (in^2)	0.348 (540)	(total area)}
Fan exhaust velocity, m/sec (ft/sec)	164.3 (539)	180.4 (592)
Core exhaust velocity, m/sec (ft/sec)	191.1 (627)	229.8 (754)
Aircraft speed, m/sec (knots)	41.2 (80)	41.2 (80)
Installed thrust, SLS, kN (lbf)	55.4 (12,462)	58.0 (13,042)

TABLE 2. - QCSEE POWERED-LIFT SYSTEM NOISE STATUS

	152-meter (500-ft) sideline EPNdB		95-EPNdB noise contour area	
	Takeoff	Approach	km^2	mi^2
QCSEE goal	95	95	1.3	0.5
NASA engine-wing test with current jet-flap technology				
UTW system	99.7	98.5	2.6	1.0
OTW system	98.4	94.6	1.3	.5

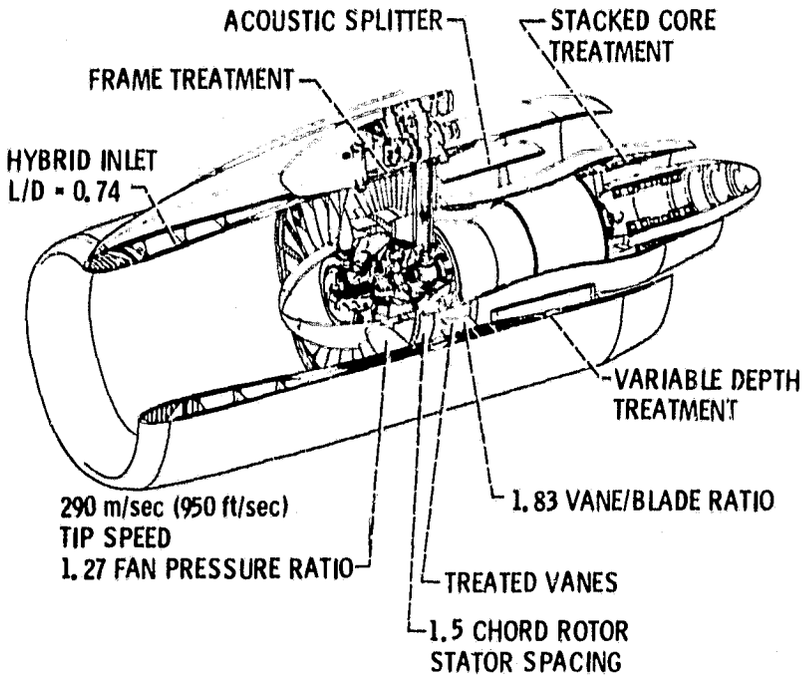

Figure 1. - UTW Engine acoustic design features.

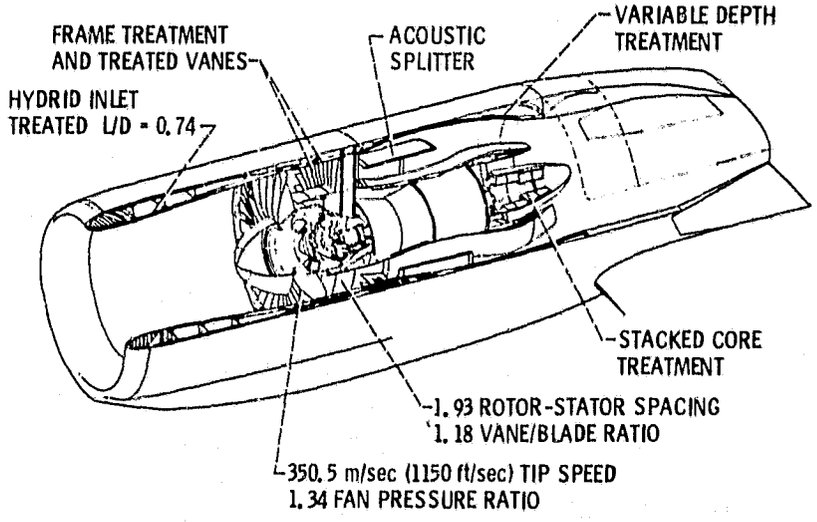

Figure 2. - OTW Engine acoustic design features.

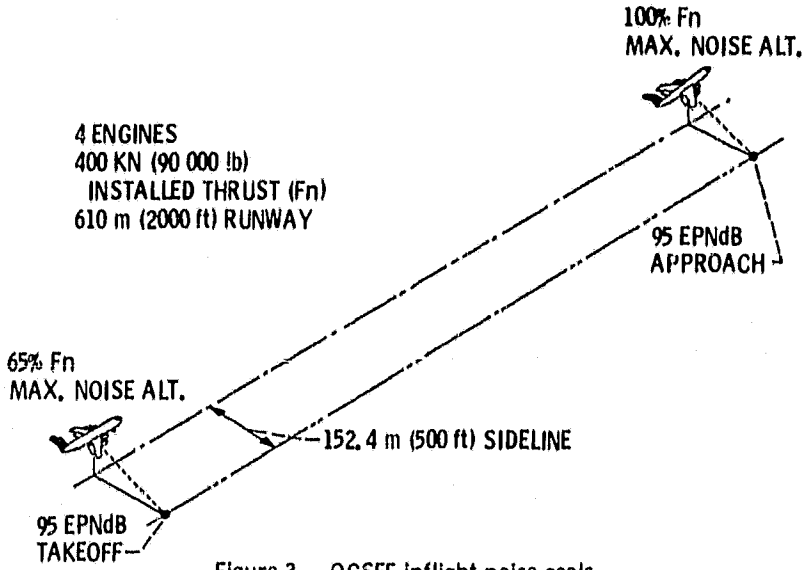

Figure 3. - QCSEE inflight noise goals.

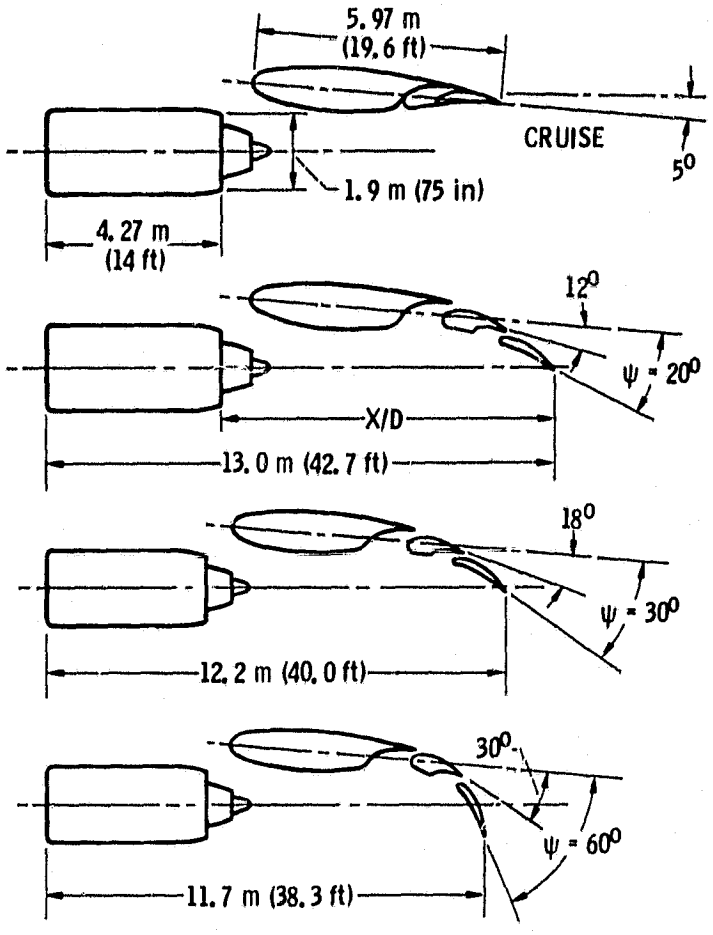

Figure 4. - UTW Wing-flap configurations.

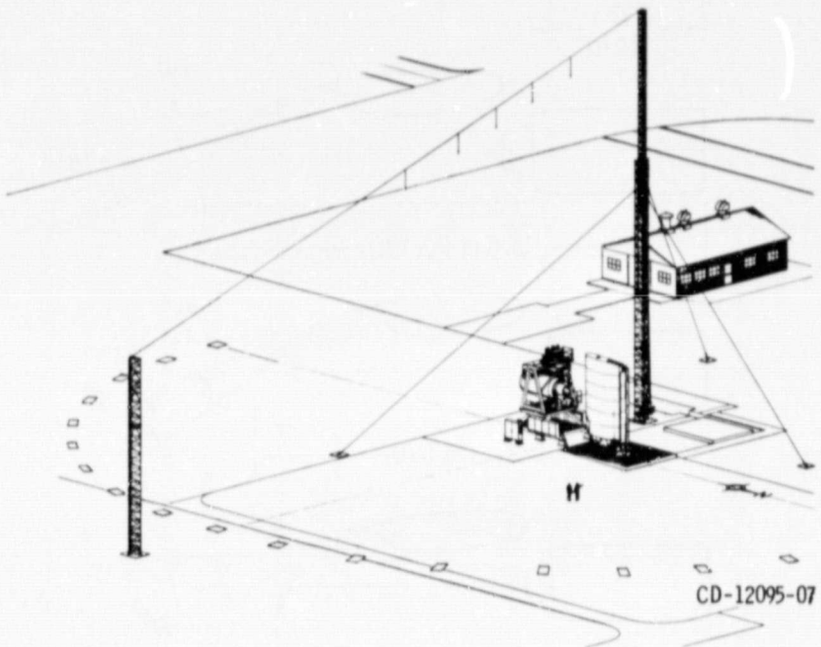

Figure 5. - Engine noise test facility showing QCSEE UTW installation and microphone towers.

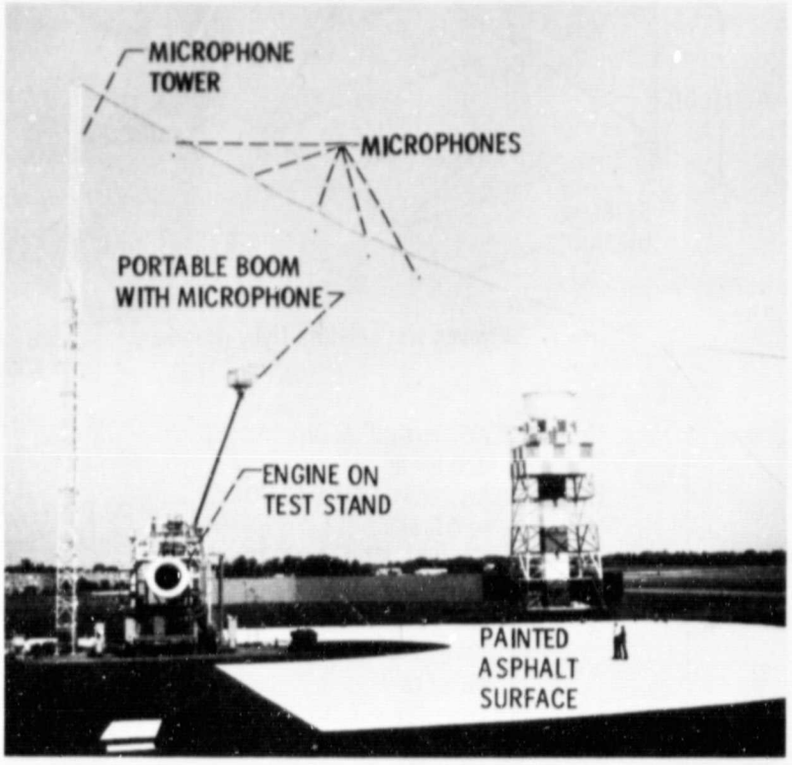

Figure 6. - Engine noise test facility showing QCSEE installation and microphone arena.

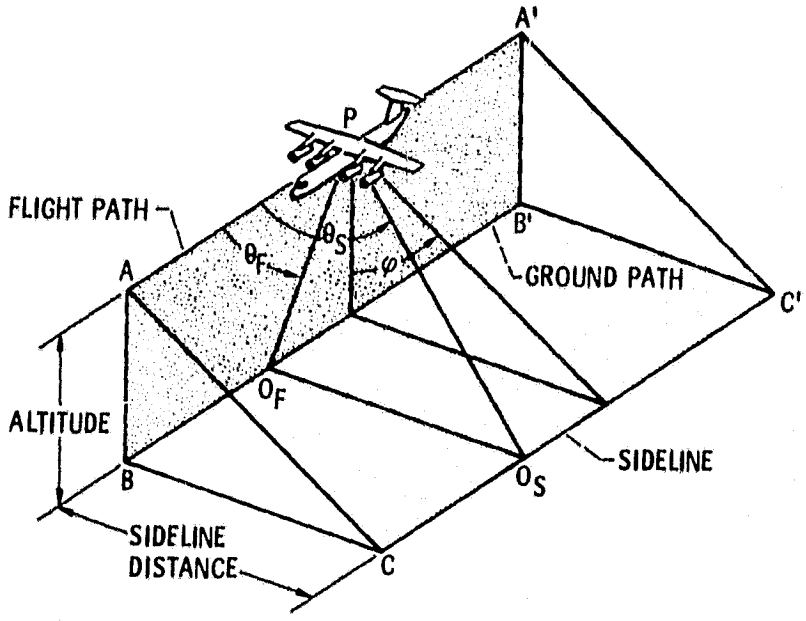

Figure 7. - Flyover and sideline flyby geometry.

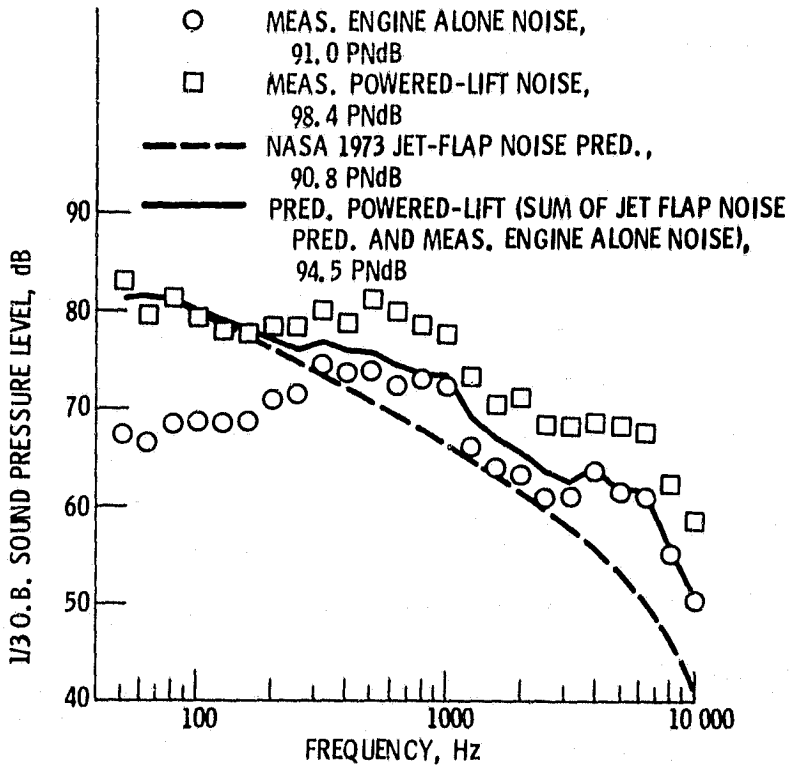

Figure 8. - Measured vs. predicted powered-lift noise take-off power, 30^0 flap angle; 152 m (500 ft) sideline at 91.4 m (300 ft) altitude.

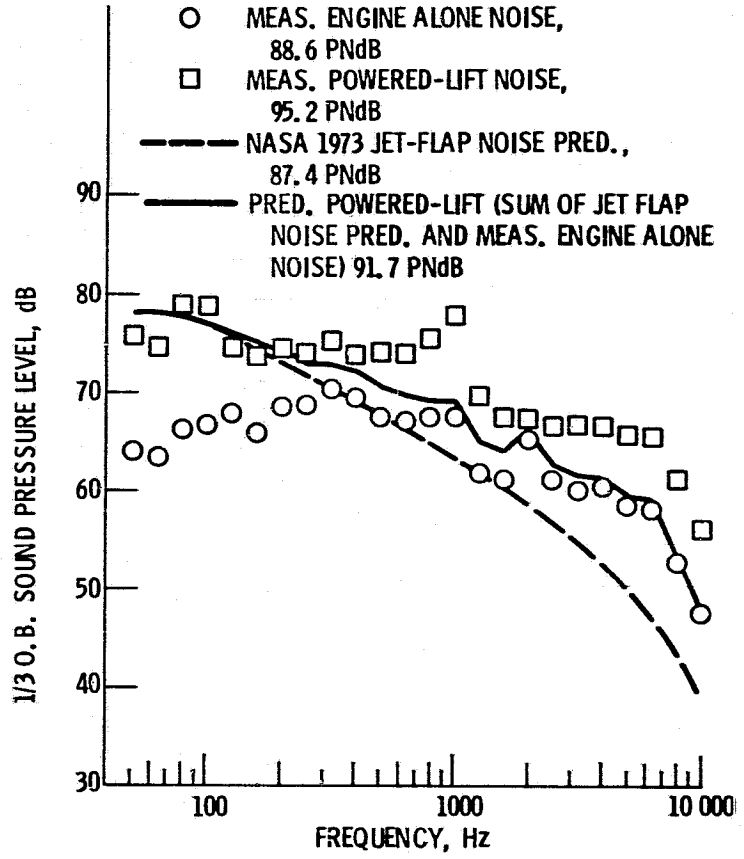

Figure 9. - Measured vs. predicted powered-lift noise approach power, 60^0 flap angle; 152 m (500 ft) sideline at 91.4 m (300 ft) altitude.

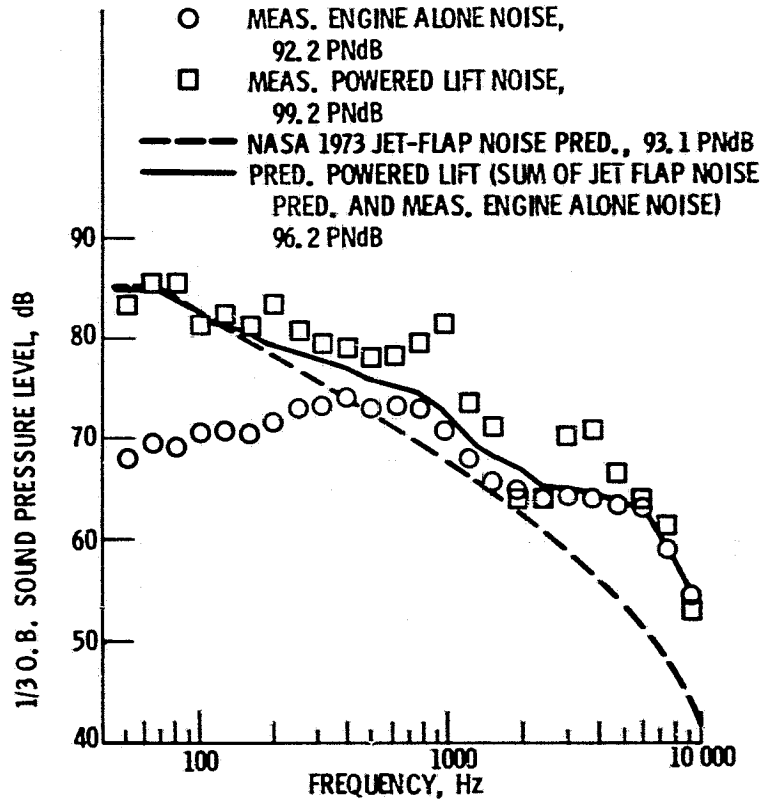

Figure 10. - Measured vs. predicted powered-lift noise: takeoff power, 30^0 flap angle; 152 m (500 ft) flyover, $\theta_F = 90^0$.

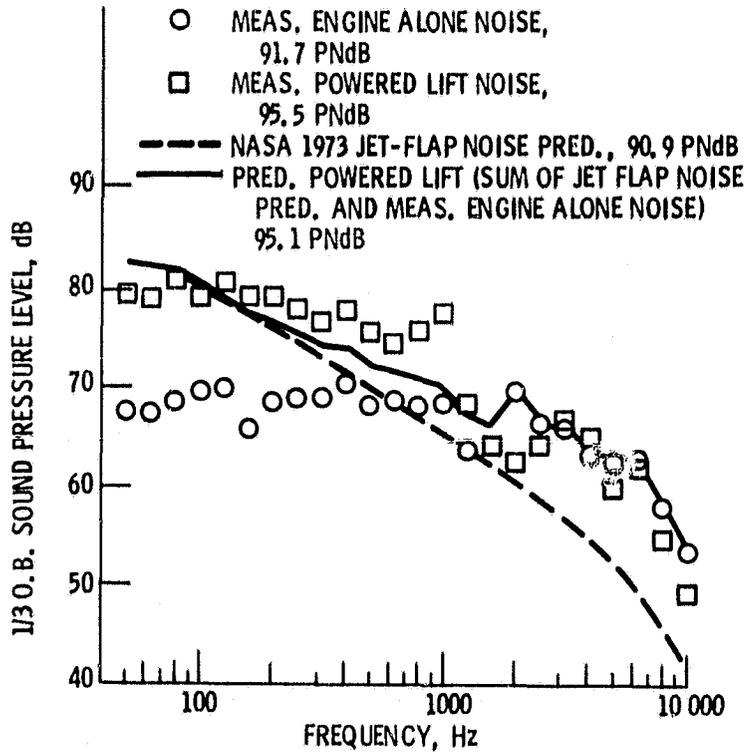

Figure 11. - Measured vs. predicted powered-lift noise: approach power, 60^{0} flap angle; 152 m (500 ft) flyover, $\theta_F = 90^{0}$.

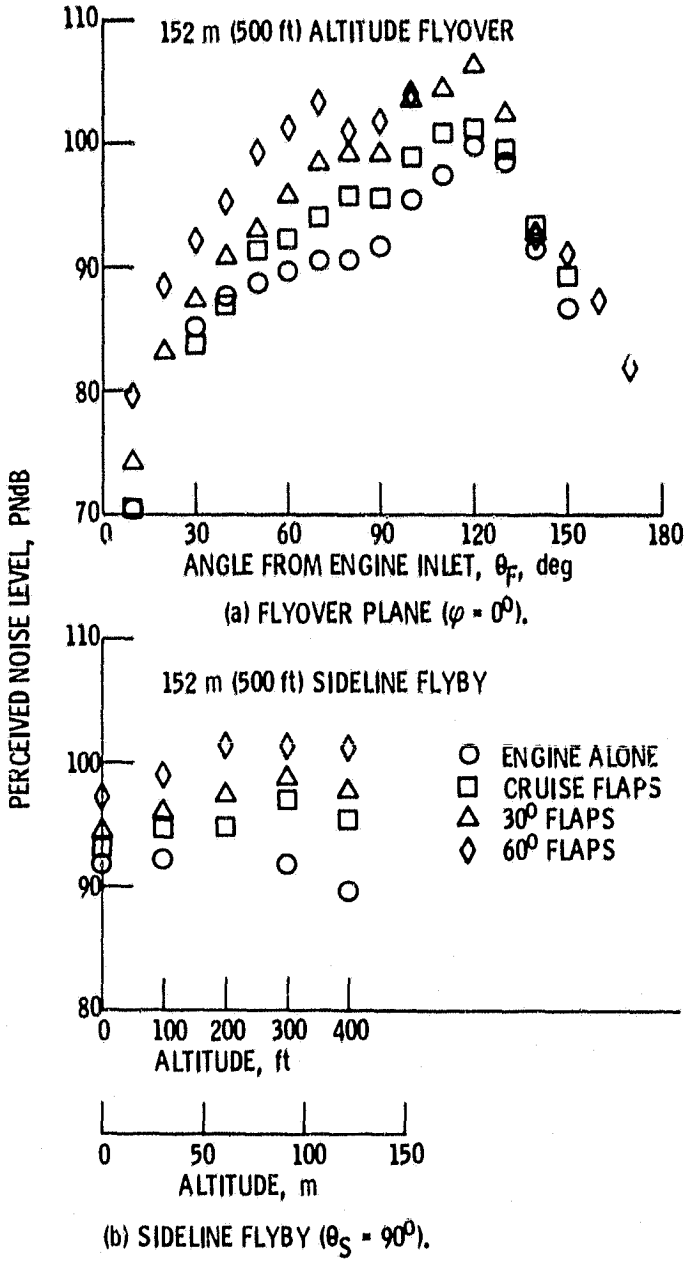

Figure 12. - Effect of flap setting on powered-lift noise: takeoff power; fully suppressed engine.

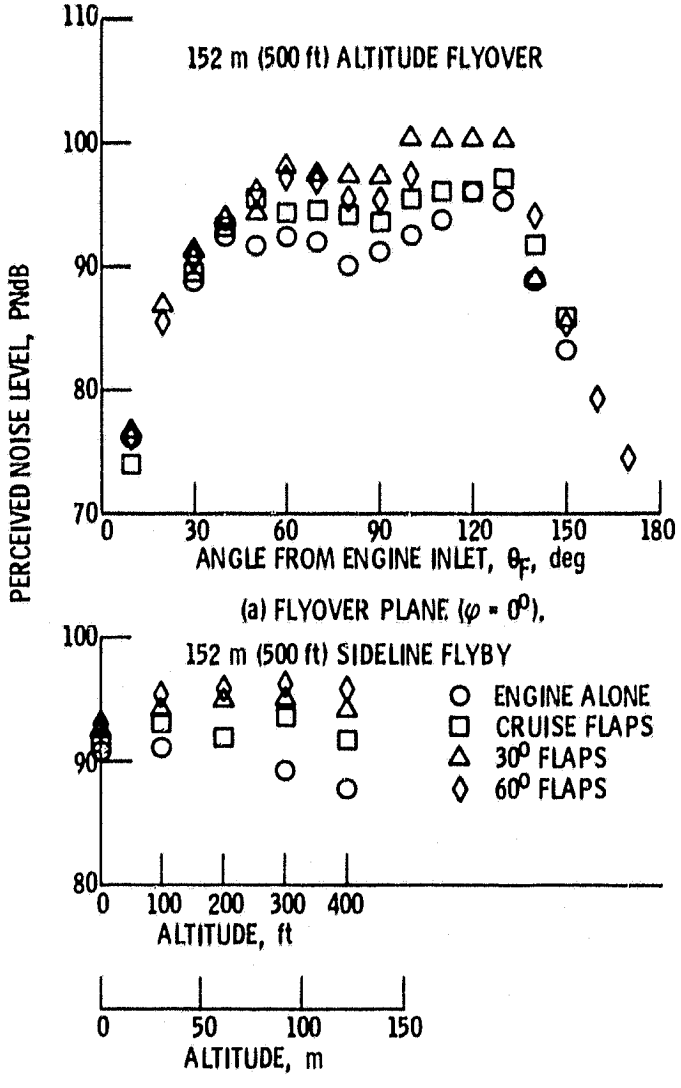

Figure 13. - Effect of flap setting on powered-lift noise: approach power; fully suppressed engine.

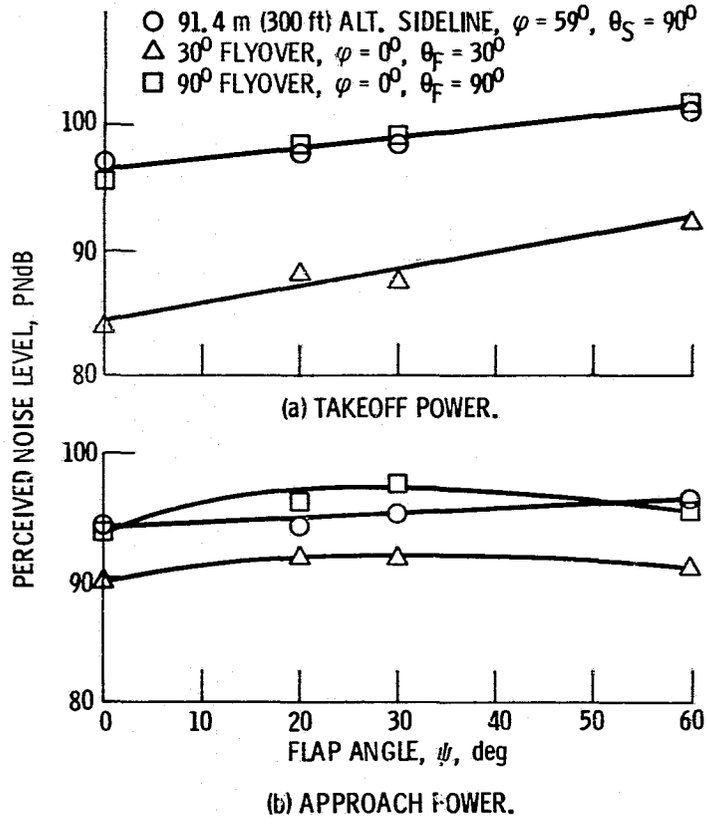

Figure 14. - Effect of flap angle on powered-lift noise; fully suppressed engine.

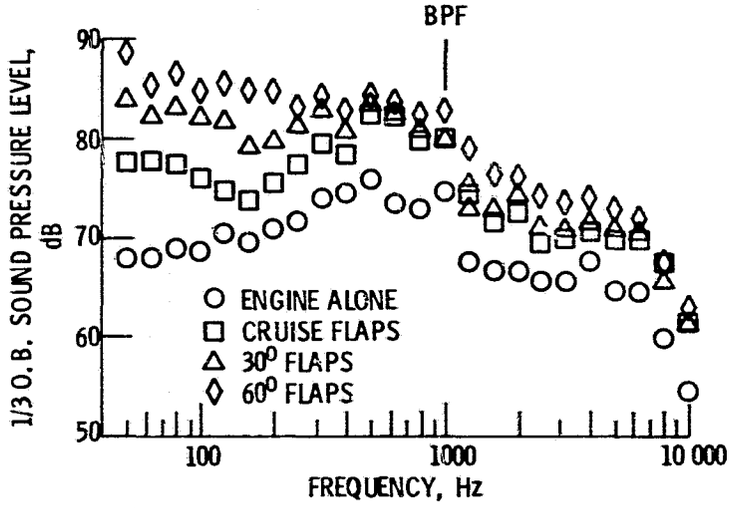

Figure 15. - Powered-lift noise spectral variation with flap angle: fully suppressed engine; takeoff power; 152 m (500 ft) sideline flyby at 91.4 m (300 ft) altitude.

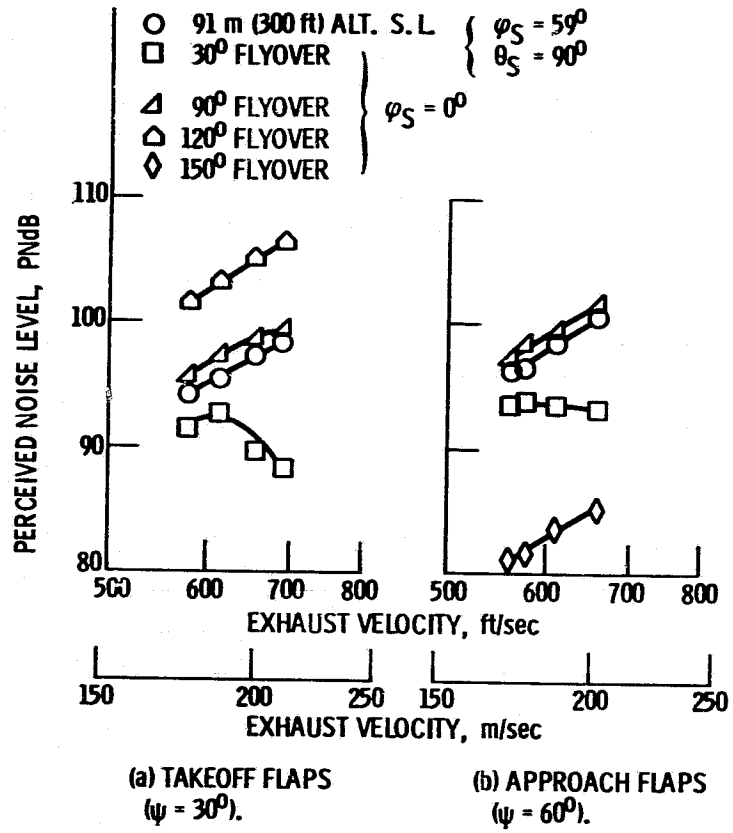

Figure 16. - UTW powered-lift noise vs. exhaust velocity; fully suppressed engine.

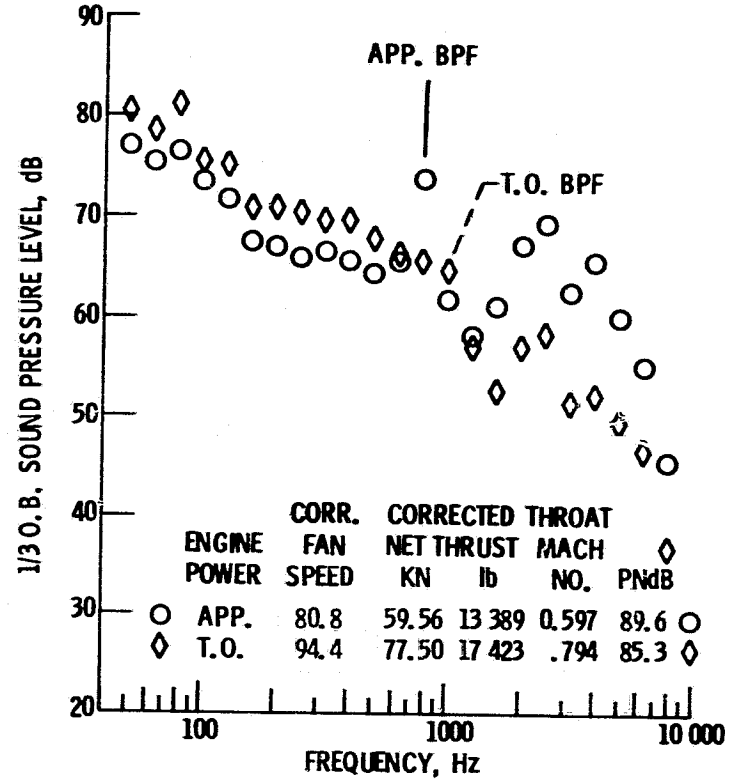

Figure 17. - Hybrid inlet suppression: fully suppressed engine; 30° flyover ($\varphi = 0^0$, $\theta_F = 30^0$).

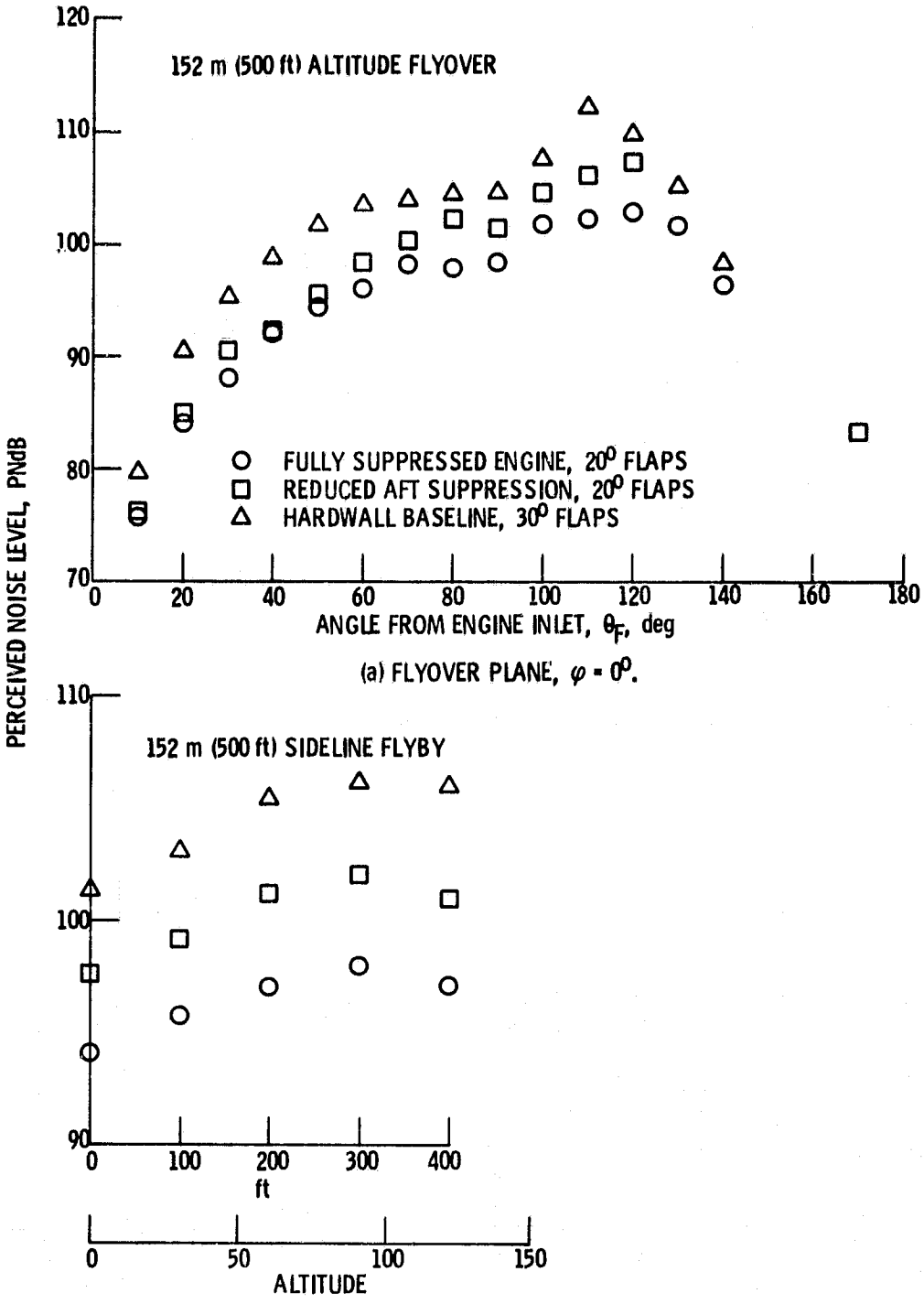

Figure 18. - Effect of reduced aft suppression on powered-lift noise. Takeoff power.

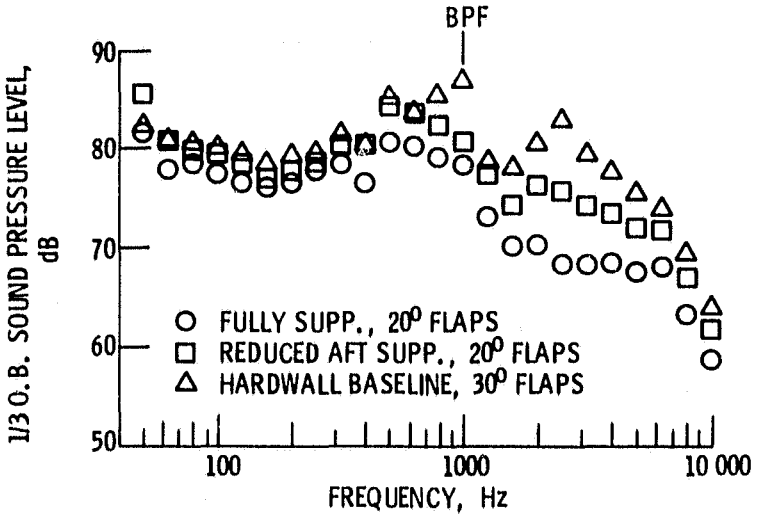

Figure 19. - Spectral effects of engine acoustic treatment: takeoff conditions; 152 m (500 ft) sideline at 91.4 m (300 ft) altitude.

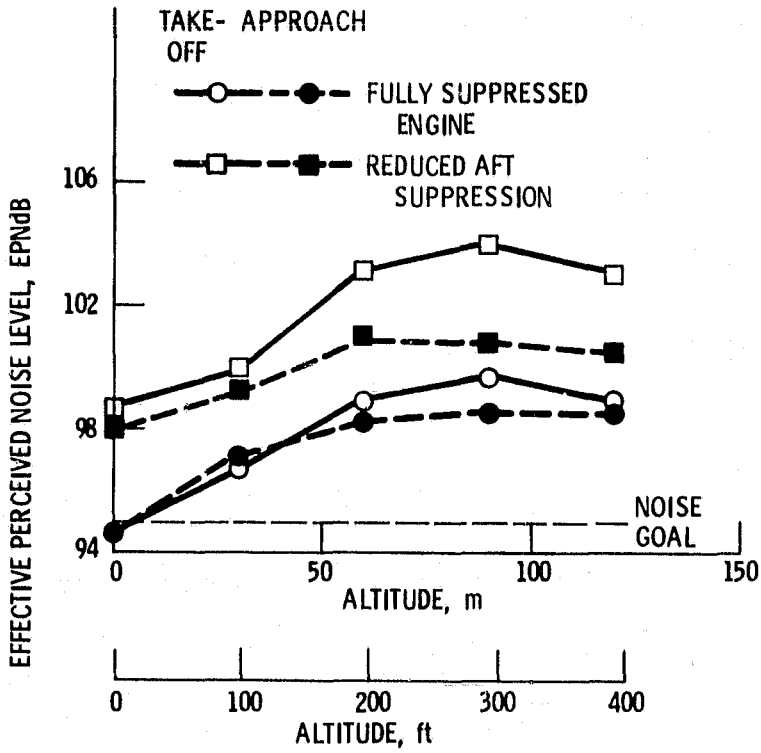

Figure 20. - QCSEE UTW inflight noise levels: 152 m (500 ft) sideline; 4 engine aircraft, 400 KN (90 000 lb) thrust.

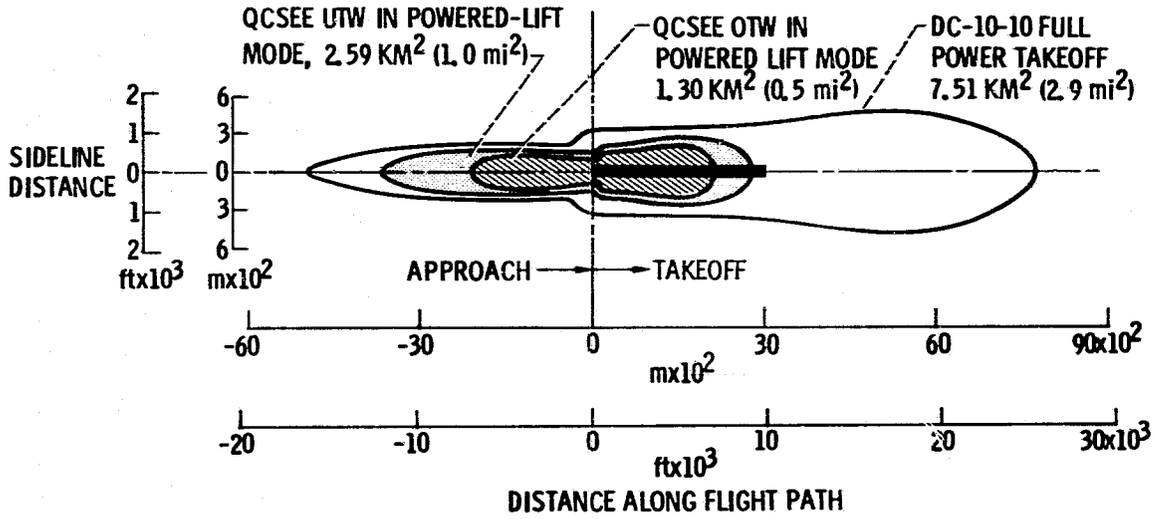

Figure 21. - EPNdB contour comparison for QCSEE and DC-10.

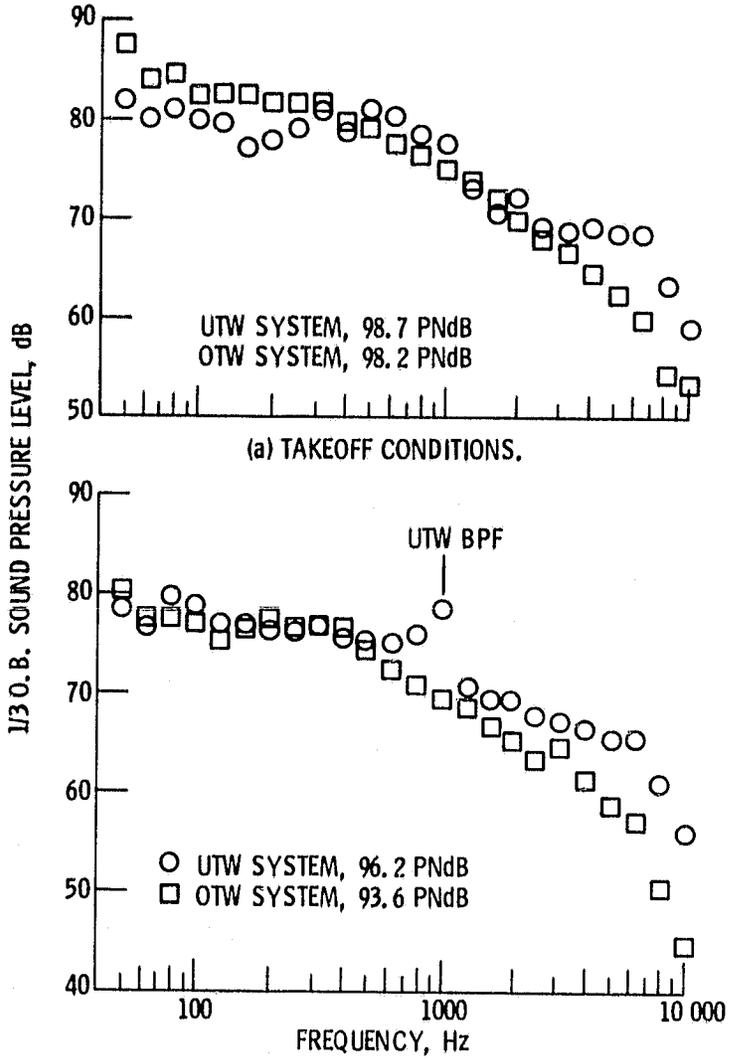

Figure 22. - Sideline noise comparison of UTW and OTW powered-lift systems. 152.4 m (500 ft) sideline at 91.4 m (300 ft) altitude.

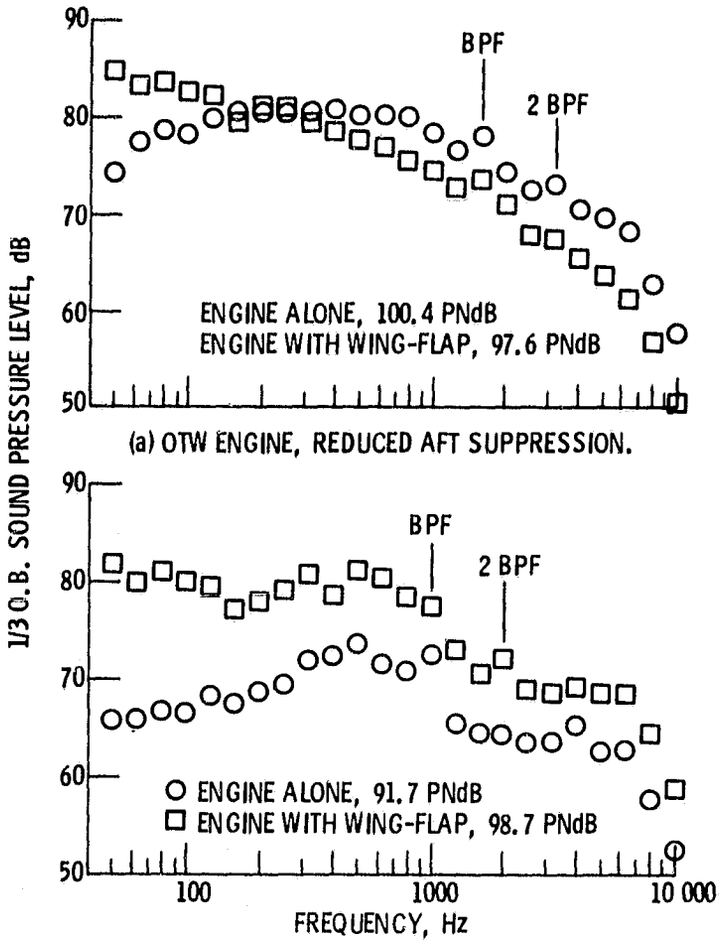

Figure 23. - Effect of wing shielding on UTW and OTW powered-lift noise takeoff conditions. 152.4 m (500 ft) sideline at 91.4 m (300 ft) altitude.